

Intrinsic Correlation of Galaxy Shapes: Implications for Weak Lensing Measurements

Alan Heavens^{1*}, Alexandre Refregier^{2†} & Catherine Heymans^{1‡}

¹ *Institute for Astronomy, Univ. of Edinburgh, Royal Observatory, Blackford Hill, Edinburgh, EH9 3HJ, UK*

² *Institute of Astronomy, Madingley Road, Cambridge CB3 0HA, UK*

Accepted —. Received —; in original form —.

ABSTRACT

Weak gravitational lensing is now established as a powerful method to measure mass fluctuations in the universe. It relies on the measurement of small coherent distortions of the images of background galaxies. Even low-level correlations in the intrinsic shapes of galaxies could however produce a significant spurious lensing signal. These correlations are also interesting in their own right, since their detection would constrain models of galaxy formation. Using $3 \times 10^4 - 10^5$ halos found in N-body simulations, we compute the correlation functions of the intrinsic ellipticity of spiral galaxies assuming that the disk is perpendicular to the angular momentum of the dark matter halo. We also consider a simple model for elliptical galaxies, in which the shape of the dark matter halo is assumed to be the same as that of the light. For deep lensing surveys with median redshifts ~ 1 , we find that intrinsic correlations of $\sim 10^{-4}$ on angular scales $\theta \sim 0.1 - 10'$ are generally below the expected lensing signal, and contribute only a small fraction of the excess signals reported on these scales. On larger scales we find limits to the intrinsic correlation function at a level $\sim 10^{-5}$, which gives a (model-dependent) range of separations for which the intrinsic signal is about an order of magnitude below the ellipticity correlation function expected from weak lensing. Intrinsic correlations are thus negligible on these scales for dedicated weak lensing surveys. For wider but shallower surveys such as SuperCOSMOS, APM and SDSS, we cannot exclude the possibility that intrinsic correlations could dominate the lensing signal. We discuss how such surveys could be used to calibrate the importance of this effect, as well as study spin-spin correlations of spiral galaxies.

Key words: cosmology: observations – gravitational lensing, galaxies: formation – statistics – fundamental parameters

1 INTRODUCTION

Weak gravitational lensing is now established as a powerful method to directly measure the distribution of mass in the universe (Gunn 1967, Blandford et al 1991, Villumsen 1996, Bernardeau 1997, Schneider et al 1998; for recent reviews see Mellier 1999; Kaiser 1999; Bartelmann & Schneider 1999). This method is based on the measurement of the coherent distortions that lensing induces on the observed shapes of background galaxies. It is routinely used to map the mass of clusters of galaxies (see Fort & Mellier 1994, Schneider 1996 for reviews) and has now been applied to a supercluster of galaxies (Kaiser et al. 1998) and to galaxy groups (Hoek-

stra et al. 1999). Recently, several groups have reported the statistical detection of weak lensing by large-scale structure (Wittman et al. 2000; van Waerbeke et al. 2000; Bacon, Refregier & Ellis 2000; Kaiser, Wilson & Luppino 2000). These detections offer remarkable prospects for precise measurements of the mass power spectrum and of cosmological parameters (Kaiser 1992; Jain & Seljak 1997; Kamionkowski et al. 1997; Kaiser 1998; Hu & Tegmark 1998; Van Waerbeke et al. 1998).

A potential limitation of this technique is the correlation of the intrinsic shapes of galaxies which would produce spurious lensing signals. These intrinsic shape correlations must therefore be accounted for in weak lensing surveys. In addition, they are interesting in their own right as their detection would constrain models of galaxy formation. Such intrinsic correlations could be produced by several effects: correlations of torques in random gaussian fields during linear evolution (e.g. Heavens & Peacock 1988), the coupling

* afh@roe.ac.uk

† ar@ast.cam.ac.uk

‡ cech@roe.ac.uk

of angular momentum of halos during their non-linear collapse (e.g. Navarro & Steinmetz 1997), tidal interaction of nearby galaxies and interaction of the galaxies with the gravitational potential from surrounding large scale structures (West, Villumsen & Dekel 1991, Tormen 1997).

A calculation of intrinsic shape correlation thus requires an understanding of the origin and properties of the angular momentum of galaxies, a problem which has puzzled astrophysicists for over 5 decades (see Efstathiou & Silk 1983 for a review). Hoyle (1949) was the first to suggest that it arises from the tidal fields of neighbouring galaxies. Peebles (1969) examined this theory by computing the growth rate of angular momentum for a spherical collapse using a second-order expansion. Doroshkevich (1970) recognised that galaxy spin emerges through first-order terms if a non-spherical halo was considered, and White (1984) showed that the resulting growth rate was linear in time. The statistics of galaxy spins arising from tidal torques on density peaks have been studied analytically and using N-body simulations (Heavens & Peacock 1988; Catalan & Theuns 1996; Barnes & Efstathiou 1987; Sugerma, Summers & Kamionkowski 1999; Lee & Pen 2000 and references therein).

In this paper, we study the correlation of galaxy shapes, quantify its impact on weak lensing surveys and assess its detectability using wide shallow surveys. We concentrate on spiral galaxies, and assume that their disk is perpendicular to the angular momentum vector of their halo. We compute the correlation of the angular momenta of halo pairs found in N-body simulations. This allows us to compute the angular correlation function of the ellipticity of the galaxies projected on the sky. We compare this intrinsic ellipticity correlation function to that expected for weak lensing surveys. In addition, we study its detectability with present and upcoming wide shallower surveys such as SuprCOSMOS, APM and SDSS. Studies of intrinsic shape correlations using analytical techniques will be presented in Crittenden et al. (2000) and Catelan, Kamionkowski & Blandford (2000); a very similar independent numerical study by Croft & Metzler (2000) has also been completed, while a detection of intrinsic spin correlations has been reported by Pen, Lee & Seljak (2000).

This paper is organised as follows. In §2, we define the ellipticity of galaxies and the associated correlation function. In §3, we compute the ellipticity correlation expected for lensing. We compute that arising from intrinsic shape correlations of galaxies in §4. In §5, we discuss the impact of the intrinsic correlation on weak lensing measurements and its detectability with wide shallow surveys. In §6, we summarise our conclusions.

2 ELLIPTICITY CORRELATION FUNCTION

Following lensing conventions, we characterise the shape of the images of galaxies on the sky by defining the ellipticity vector $\epsilon_i = \{\epsilon_1, \epsilon_2\}$ as

$$\epsilon_i = \frac{a^2 - b^2}{a^2 + b^2} \{\cos 2\alpha, \sin 2\alpha\} \quad (1)$$

where a and b are the major and minor axes of the galaxy image, and α is its position angle counter-clockwise from the x-axis. The ellipticity is independent of the surface brightness profile, provided only that the projected contours of

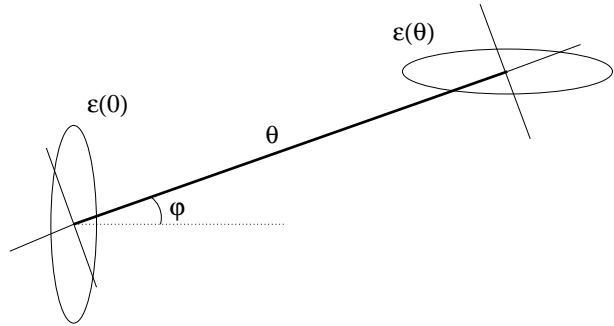


Figure 1. Geometry of the ellipticity correlation functions. Two galaxies separated by an angle θ are assigned ellipticities $\epsilon_i(0)$ and $\epsilon_i(\theta)$. These ellipticities can then be transformed into the rotated ellipticities $\epsilon_i^r(0)$ and $\epsilon_i^r(\theta)$ defined in the coordinate system (thin solid lines) which is aligned with the separation vector θ . The two correlation functions are then defined as $C_1(\theta) \equiv \langle \epsilon_1^r(0)\epsilon_1^r(\theta) \rangle$ and $C_2(\theta) \equiv \langle \epsilon_2^r(0)\epsilon_2^r(\theta) \rangle$

surface brightness are elliptical. The ellipticity component ϵ_1 (ϵ_2) corresponds to elongation and compressions along (at 45° from) the x-axis. Under a rotation of the coordinate system by an angle φ (counter-clockwise from the original x-axis), the ellipticity ϵ_i transforms into the rotated ellipticity ϵ_i^r given by

$$\epsilon_i^r = R_{ij}(2\varphi)\epsilon_j, \quad (2)$$

where the rotation matrix is defined as

$$R_{ij}(2\varphi) = \begin{pmatrix} \cos(2\varphi) & \sin(2\varphi) \\ -\sin(2\varphi) & \cos(2\varphi) \end{pmatrix}. \quad (3)$$

The correlation of the shapes of galaxy images can be quantified using the ellipticity correlation functions. Let us consider two galaxy images separated by an angular vector θ , with ellipticities $\epsilon_i(0)$ and $\epsilon_i(\theta)$. The geometry of the correlation functions is illustrated in Figure 1. It is convenient to consider a coordinate system which is rotated so that its x-axis is aligned with the separation vector θ . In this rotated coordinate system, the ellipticities of the two galaxies are $\epsilon_i^r(0)$ and $\epsilon_i^r(\theta)$ and can be derived from equation (2) with φ set to the angle between θ and the positive x-axis. We can then define the rotated ellipticity correlation functions (Miralda-Escudé 1991, Kaiser 1992)

$$\begin{aligned} C_1(\theta) &= \langle \epsilon_1^r(0)\epsilon_1^r(\theta) \rangle \\ C_2(\theta) &= \langle \epsilon_2^r(0)\epsilon_2^r(\theta) \rangle, \end{aligned} \quad (4)$$

where the brackets denote an average over pairs of galaxies separated by an angle θ . The correlation functions $\langle \epsilon_1^r(0)\epsilon_2^r(\theta) \rangle$ and $\langle \epsilon_2^r(0)\epsilon_1^r(\theta) \rangle$ are expected to vanish since they flip sign under a parity transformation ($x \rightarrow -x, y \rightarrow y$). In the following section, we compute the amplitude of these correlation functions expected from weak lensing. The predictions for $C_1(\theta)$ and $C_2(\theta)$ from intrinsic correlations will be presented in §4.

3 CORRELATIONS FROM WEAK LENSING

Weak gravitational lensing produces coherent distortions in the images of background galaxies (see Mellier 1999; Kaiser 1999; Bartelmann & Schneider 1999 for recent reviews).

This effect is characterized by the distortion matrix $\Psi_{ij} \equiv \partial(\delta\theta_i)/\partial\theta_j$ where $\delta\theta_i(\theta_j)$ is the angular displacement field induced by lensing at position θ_j . The trace free part of the distortion matrix is called the shear $\gamma_i \equiv \{\Psi_{11} - \Psi_{22}, 2\Psi_{12}\}/2$ and can be directly measured from the ellipticity of background galaxies (if they are intrinsically uncorrelated). For the definition of ellipticity in Equation (1) and in the weak lensing regime, the shear is indeed related to the average galaxy ellipticity by e.g. Rhodes et al. (1999).

$$\gamma_i = \langle \epsilon_i \rangle / \lambda, \quad (5)$$

where the brackets denote an average over randomly oriented galaxies, $\lambda \equiv 2(1 - \sigma_\epsilon^2)$, and $\sigma_\epsilon^2 \equiv \langle \epsilon_1^2 \rangle = \langle \epsilon_2^2 \rangle$ is the ellipticity variance of the galaxies in the absence of lensing. In the following, we will adopt $\sigma_\epsilon \simeq 0.3$ as is typically found in weak lensing surveys (e.g. Rhodes et al. 1999; Bacon et al. 2000), yielding $\lambda \simeq 1.8$.

For weak lensing, the ellipticity correlation functions (Eq. [4]) are given by (Miralda-Escudé 1991, Kaiser 1992, Kamionkowski et al. 1997; Bacon, Refregier & Ellis 2000)

$$C_i(\theta) = \frac{\lambda^2}{4\pi} \int_0^\infty dl l C_l^\gamma [J_0(l\theta) + (-1)^{i+1} J_4(l\theta)], \quad (6)$$

where C_l^γ is the shear power spectrum given by (e.g. Bacon, Refregier & Ellis 2000)

$$C_l^\gamma = \frac{9}{16} \left(\frac{H_0}{c}\right)^4 \Omega_m^2 \int_0^\infty d\chi \left[\frac{g(\chi)}{a r(\chi)}\right]^2 P\left(\frac{l}{r}, \chi\right), \quad (7)$$

where $P(k, \chi)$ is the 3-dimensional mass power spectrum at comoving radius χ and a is the scale factor normalised to unity today. The comoving angular-diameter distance is $r(\chi) = R_0 \sinh(\chi R_0^{-1})$, χ , and $R_0 \sin(\chi R_0^{-1})$, in an open, flat and closed universe respectively. The scale radius at present is $R_0 = c/(\kappa H_0)$, with $\kappa^2 = 1 - \Omega$, 1, and $\Omega - 1$, in each case respectively. The radial weight function $g(\chi)$ is given by

$$g(\chi) = 2 \int_\chi^\infty d\chi' p_\chi(\chi') \frac{r(\chi)r(\chi' - \chi)}{r(\chi')}. \quad (8)$$

The selection function $p_\chi(\chi)$ is the probability that an object at radius χ is included in the catalogue and is normalised as

$$\int d\chi p_\chi(\chi) \equiv 1. \quad (9)$$

It is related to the redshift probability function p_z by $p_\chi d\chi = p_z dz$. We will consider a redshift distribution of the form

$$p_z(z) \propto z^2 \exp\left[-\left(\frac{z}{z_0}\right)^\beta\right], \quad (10)$$

which gives an approximate description of the observed distribution for $\beta \simeq 1.5$ (e.g. Smail et al. 1995). The mean and median redshift of this distribution are $\langle z \rangle \simeq 1.5z_0$ and $z_m \simeq 1.4z_0$, respectively. We will consider two distributions with $z_m = 1.0$ and $z_m \simeq 0.2$, corresponding, respectively, to that for current weak lensing surveys and for wide but shallower surveys such as SuperCOSMOS, APM and SDSS (Maddox et al. 1990, Gunn & Weinberg 1995).

Figure 2 (dotted lines) shows the correlation functions expected for lensing for the cosmological models of Table 1. They were derived using the fitting formula of Peacock and Dodds (1996) for the non-linear evolution of the mass power spectrum. The redshift distribution of the sources was taken

Table 1. Cosmological models

Model	Ω_m	Ω_Λ	σ_8	Γ
SCDM	1.0	0	0.51	0.50
τ CDM	1.0	0	0.51	0.21
LCDM	0.3	0.7	0.90	0.21
OCDM	0.3	0	0.85	0.21

to be that of Equation (10) with $z_m = 1$. Note that these correlation functions have a specific angular dependence which can be used as a signature of lensing. In particular, C_2 turns negative for $\theta \gtrsim 20'$ (not shown) for all models (Miralda-Escudé 1991, Kaiser 1992, Kaiser 1998; Kamionkowski et al. 1998).

Figure 3 shows an example of the lensing correlation function for a median redshift of $z_m = 0.2$. We see that the amplitude is more than one order of magnitude lower than that for $z_m = 1$. This reflects the fact that lensing produces coherent ellipticities throughout the depth of the survey. It is therefore advantageous to use deep surveys to detect lensing. This is in contrast to intrinsic correlations which are expected to be important on small spatial scales, and thus be diluted when averaged over the depth of deep lensing surveys. This is reflected to a certain extent in the figure, but we do not have enough pairs at small physical separation to constrain the intrinsic signal for shallow surveys.

4 INTRINSIC CORRELATIONS

4.1 Galaxy Models

We have considered two galaxy models, ‘ellipticals’ and ‘spirals’, based on halos identified in N-body simulations. Our elliptical model is similar to that considered by Croft & Metzler (2000) and assumes that the ellipticity of the galaxy is the same as the ellipticity of the dark matter halo; since the halos contain rather few particles (10-146), we are not confident that the true halo ellipticity is computed accurately, due to possible numerical artefacts. We thus concentrate on a model for spiral galaxies, for which we use the angular momentum of the halo, not its shape. The fraction of spirals in the field population is high, although observationally sample-dependent (e.g. Loveday et al. 1992, Lin et al. 1996, Folkes et al. 1999), which also motivates our choice.

We model a spiral galaxy as a thin disk which is assumed to be perpendicular to the angular momentum vector \mathbf{L} of its parent halo. The geometry of such a disk is shown in Fig. 5. Let us choose a coordinate system such that the sky is in the x - y plane, and the line of sight is along the z -axis. Let us call the polar angle and the azimuthal angle of \mathbf{L} in this coordinate system as μ and ν , respectively. The disk is shown as the open ellipse on the figure, and its projection on the sky as the filled ellipse. It is easy to show that the ellipticity $\epsilon \equiv (\epsilon_1^2 + \epsilon_2^2)^{1/2}$ and position angle α of the projected ellipse (eq. [1]) are given by

$$\begin{aligned} \epsilon &= \frac{\sin^2 \mu}{1 + \cos^2 \mu}, \\ \alpha &= \nu + \frac{\pi}{2}. \end{aligned} \quad (11)$$

Note that the observed ellipticity ϵ_i depends only on the

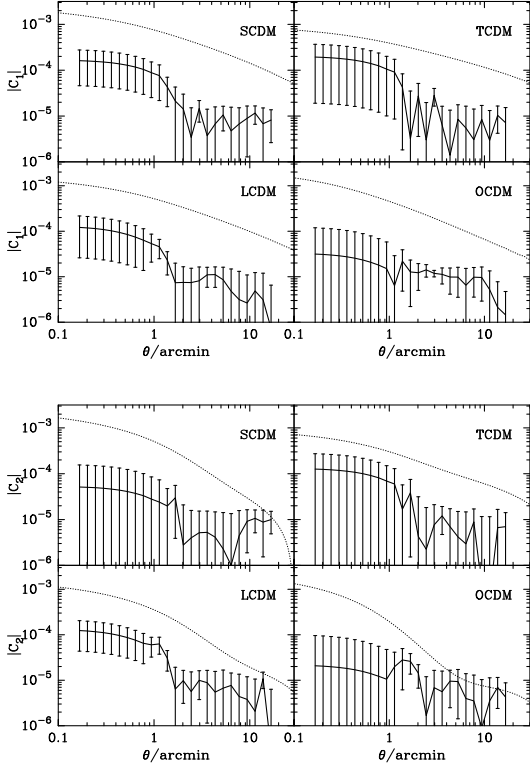


Figure 2. Intrinsic ellipticity correlation functions $|C_1(\theta)|$ (top group) and $|C_2(\theta)|$ (bottom group) for spiral galaxies, for each cosmological model. The correlation functions expected from lensing are shown as dotted lines. The source redshift was taken to be $z_s = 1$, corresponding to current dedicated weak lensing surveys. Note that error bars are correlated.

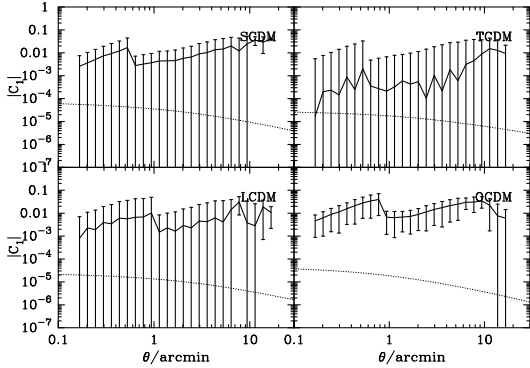


Figure 3. Same as the top group of the previous figure, but for a median galaxy redshift of $z_m = 0.2$, as appropriate for wide shallower surveys such as SDSS. We have too few small-separation pairs to constrain the intrinsic correlations between close pairs on the sky in a shallow survey. Note that error bars are correlated; most of the estimate comes from the first two bins in 3D, and the final panel is not a significant detection, since it is a log scale.

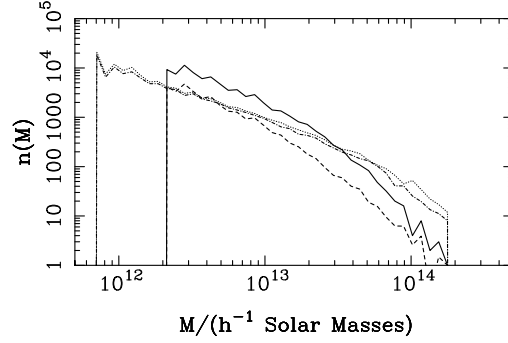


Figure 4. Mass histograms for the halos in the 4 model boxes, with 50 bins equally-spaced logarithmically. Minimum mass is set by requiring halos to have at least 10 particles. The maximum mass we consider in the analysis is $10^{13} h^{-1} M_\odot$.

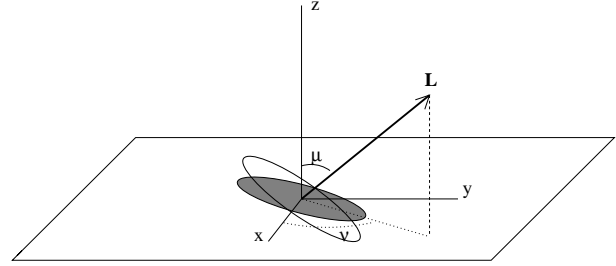


Figure 5. Simple model of a spiral galaxy which is taken to be a thin disk perpendicular to its angular momentum vector \mathbf{L} . The coordinate system is chosen so that the sky is in the x - y plane and the line of sight is along the z -axis. The disk of the galaxy is shown as the open ellipse, and its projection on the sky as the filled ellipse.

orientation of \mathbf{L} , and not on its magnitude; it is also independent of the surface brightness profile, provided it depends only on radius. The ‘elliptical’ model assigns ellipticities from the halo quadrupole moments as discussed in Kaiser & Squires (1993).

4.2 Simulations

We use N-body simulations developed by the Virgo Consortium (Jenkins et al. 1998) for the 4 cosmological models with parameters listed in table 1. The simulations have 256^3 particles, box sizes of $239.5 h^{-1}$ Mpc, and use a parallel, adaptive particle-particle, particle-mesh scheme ($h \equiv H_0/100 \text{ km s}^{-1} \text{ Mpc}^{-1}$). We have one simulation per cosmological model. Halos are found using a friends-of-friends algorithm, with a linking length of 0.2 times the mean particle separation. In each simulation, we identify about $3 \times 10^4 - 1.2 \times 10^5$ dark matter halos, dependent on the model, containing at least 10 particles, and with masses under $10^{13} h^{-1} M_\odot$ and measure their angular momenta. The minimum mass is $6.9 \times 10^{11} h M_\odot$ for low-density models and $2.3 \times 10^{12} h M_\odot$ for high-density models. Mass distributions are shown in Fig. 4. We choose one side of the box as the plane of the sky and compute the ellipticity of a disk at right-angles to the halo angular momentum, using Equation (11).

Since we assume the disks to be thin, the magnitude of the angular momentum is irrelevant. There is a possibility of angular momentum transfer between the baryon component and the halo, through sub-clumps coupling to the halo potential (e.g. Navarro & Steinmetz 1997), but we assume no change in the direction of \mathbf{L} . We then select pairs of halos and compute the 3-dimensional ellipticity correlation functions

$$\begin{aligned}\eta_1(r) &\equiv \langle \epsilon_1^r(0)\epsilon_1^r(r) \rangle \\ \eta_2(r) &\equiv \langle \epsilon_2^r(0)\epsilon_2^r(r) \rangle,\end{aligned}\quad (12)$$

where the superscript r denotes rotated ellipticities (Eq. [2]), and r is the comoving distance between the two galaxies. Strictly speaking, the correlation functions depend on the orientation of the radius vector with respect to the line-of-sight, but we average over this angular dependence. For a projected catalogue, this averaging will be a good approximation for small separations (\ll the scale over which the selection function changes), as the pairs in the catalogue will be distributed more-or-less isotropically. Figures 6 and 7 show the resulting 3-dimensional correlation functions for the LCDM model at redshift 1, for spirals and ellipticals respectively. A small but significant signal is detected on scales smaller than a few Mpc. The other models yield similar results. A useful test is that $\langle \epsilon_1^r(0)\epsilon_2^r(r) \rangle$ and $\langle \epsilon_2^r(0)\epsilon_1^r(r) \rangle$ are always consistent with zero (lower panels), as demanded by parity considerations. In the next section, we use these results to compute the projected ellipticity correlation function.

4.3 Ellipticity Correlation Functions

Since the halo 3D correlation functions (η_1 and η_2), are rotationally invariant by construction, we can compute the observed 2-dimensional intrinsic correlation functions C_1^{int} and C_2^{int} (Eq. [4]) by integration. Since the observed correlation functions are pair-weighted, we obtain

$$C_i^{\text{int}}(\theta) \simeq \frac{\int_0^\infty d\chi_1 \int_0^\infty d\chi_2 p_\chi(\chi_1)p_\chi(\chi_2)[1 + \xi(r_{12})]\eta_i(r_{12})}{\int_0^\infty d\chi_1 \int_0^\infty d\chi_2 p_\chi(\chi_1)p_\chi(\chi_2)[1 + \xi(r_{12})]} \quad (13)$$

where χ is the comoving radius, and $\xi(r)$ is the spatial correlation function of the galaxy positions. We assume $\xi(r) = (r/5h^{-1}\text{Mpc})^{-1.8}$ and ignore evolution, in view of the weak evolution seen in galaxy samples since a redshift of 3 (Giavalisco et al. 1998). Similarly, the 3D ellipticity correlation will in general evolve with time. In fact we see little difference with epoch. For the lensing of a background with median redshift $z_m = 1$, we take the halos from simulations at $z = 1$. For the shallower samples with $z_m = 0.2$, we use the correlation function from simulations at $z = 0$.

Equation (13) could be simplified to something similar to Limber's equation for the angular correlation function (Limber 1953), but we simply integrate this expression, using the small angle approximation so the comoving distance r_{12} between the two galaxy positions is

$$r_{12}^2 \simeq (\chi_1 - \chi_2)^2 + r^2 \left(\frac{\chi_1 + \chi_2}{2} \right)^2 \theta^2, \quad (14)$$

where $r(\chi)$ is the comoving angular-diameter distance defined in §3. For the Λ model, we use r derived from a fitting formula in Pen (1999). The selection function $p_\chi(\chi)$ is that

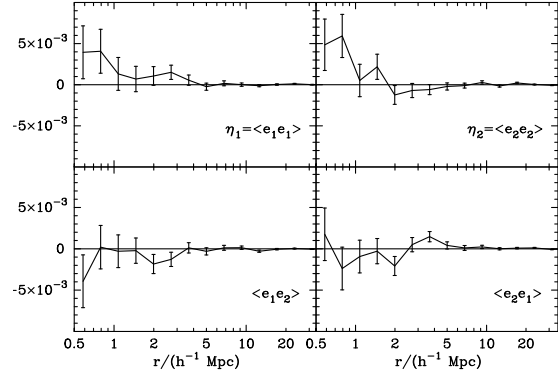


Figure 6. Three-dimensional correlation functions for spirals in the LCDM model at a redshift $z = 1$.

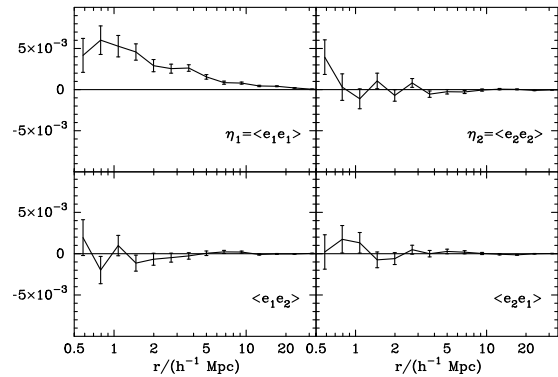


Figure 7. Three-dimensional correlation functions for ellipticals in the LCDM model at a redshift $z = 1$.

defined in equation (10). Specifically, we use the 3D ellipticity correlation function as computed from the simulations, and linearly-interpolate between points.

Figure 2 shows the resulting projected correlation functions for $z_m = 1$ for each model. We generate 50 realisations of the 3D correlation function, using the computed errors, and project, using equation (13). The resulting errors in the angular correlation function will be correlated. The case of $z_m = 0.2$ is shown in Fig. 3. Croft & Metzler (2000), using essentially the ‘elliptical’ model, present very similar results, using the LCDM model and higher-resolution, smaller simulations in addition to that used here. In Fig. 8, we present elliptical results only for the LCDM model with $z_m = 1$, which is the model they consider. Note that the elliptical correlations are less noisy than the spirals. They use higher-resolution simulations and a different algorithm for the halo-finder, and a slightly different selection function, but their results are very similar to ours. It is interesting to note that the spiral and elliptical models give very similar correlation functions. This is surprising, as there is a large scatter between the elliptical and spiral ellipticity parameters.

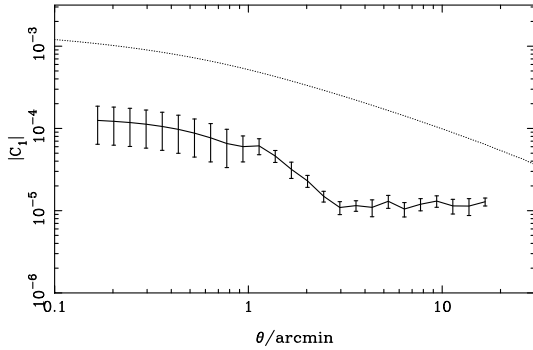


Figure 8. Intrinsic ellipticity correlation function (solid) for ellipticals in the *LCDM* model at a redshift $z = 1$, along with the expected signal from weak lensing (dotted).

5 IMPACT FOR WEAK LENSING SURVEYS AND DETECTABILITY

The impact of intrinsic correlations on current weak lensing surveys (with $z_m \sim 1$) can be established by examining figure 2. They reveal that the intrinsic correlation functions are generally below the lensing correlation functions for $\theta \lesssim 10'$. However, they are not far below for some models, and our results indicate that intrinsic shape correlations could be non-negligible.

It is interesting to note that Van Waerbeke et al. (2000) found evidence for an ellipticity variance signal in excess of lensing on $0.5' \lesssim \theta \lesssim 3.5'$ scales in their cosmic shear survey. This excess signal vanishes if galaxy pairs with separations less than $10''$ are removed. They interpret this signal as arising from overlapping isophotes, but do not dismiss the possibility that it is due to intrinsic correlations. Our results indicate that the latter explanation, although possible, is unlikely. (Note that they use a slightly different statistic, but their level of excess is in excess of our $\sqrt{C_{1,2}} \sim 0.01$).

Wider but shallower surveys such as SuperCOSMOS, APM and SDSS (Maddox et al. 1990; Gunn & Weinberg 1995) can also be used to search for weak lensing (Stebbins, McKay & Frieman 1995). Figure 3 shows the impact of intrinsic correlations on such a survey (with $z_m \sim 0.2$). In this case, the limits on the intrinsic correlations are much larger than the expected lensing signal. This can be understood in simple terms: while lensing produces correlations which are coherent through the depth of the survey, intrinsic shapes are correlated in a localised region of space. As a result, while the amplitude of lensing is smaller for shallower surveys, that for intrinsic correlations is larger, since it is not diluted as in the case of deeper surveys. Intrinsic correlations could thus be important for shallow surveys. In fact, depending on its level, and the degree of evolution, one might be able to use shallow surveys to measure the intrinsic correlation effect, and then use these results to validate or correct the correlation function derived from deep lensing surveys. Of course, the ellipticity correlation may be of intrinsic interest, possibly acting as a discriminator between cosmological models, although this looks ambitious at present.

6 CONCLUSIONS

We have studied the effect of intrinsic shape correlations on weak lensing surveys. This effect can be thought as being analogous to the foreground contributions to the anisotropy of the Cosmic Microwave Background: it must be accounted for in the interpretation of weak lensing surveys, and can provide important cosmological information in itself.

We have considered two models for the galaxies. Most of our results are based on a model for spiral galaxies, where the galaxy is assumed to be a thin disk perpendicular to the halo angular momentum. We also show some results for an ‘elliptical’ model, where we assumed that the ellipticity of the galaxy is the same as the ellipticity of the halo. The relatively small number of particles in the halos leads to some uncertainty in the shape parameters of the halo, so we have therefore concentrated on the spiral model. We measured the resulting projected ellipticity correlation function arising from spin-spin correlation of $30,000 - 10^5$ halos in an N-body simulations, for several CDM models. The correlations we find lie between $\sim 10^{-4}$ at small separations to $\sim 10^{-5}$ on scales of $10'$, and may be explicable in terms of the statistics of the initial gravitational potential (Catelan, Kamionkowski and Blandford 2000). The intrinsic correlations are generally below the expected lensing signal for deep surveys. We note that other non-gravitational effects could increase the correlations, through tidal interactions forming tidal tails, for example. However, since these effects would be confined to small separations in 3D, our feeling is that they are unlikely to be of importance in the angular correlations, especially for the deep samples.

For a survey with galaxies at a median redshift $z_m = 1$, such as current weak lensing surveys, intrinsic correlations lie below the lensing signal on angular scales $\theta \lesssim 10'$, a scale where the lensing signal is $\sim 10^{-5}$. The effect appears to be too small to explain the excess power found on small scales by Van Waerbeke et al. (2000).

While lensing produces correlations which are coherent over the depth of the survey, intrinsic shape correlations are only important over limited physical separations. As a result, intrinsic correlations are diluted when integrated over the depth of a deep, dedicated lensing survey. On the other hand, wider but shallower surveys such as SDSS ($z_m \sim 0.2$) will be much more sensitive to intrinsic correlations. We cannot exclude the possibility that intrinsic correlations could be comparable to or even dominate the weak lensing signal on all scales for such surveys. Caution must thus be exerted when interpreting the weak lensing signal from these surveys. With sufficient signal, the lensing signal can be secured using the specific angular dependence of its induced ellipticity correlations, but shot noise will be a strong limiting factor at scales of an arcminute or less in a survey like SDSS (see Munshi and Coles 2000 for further discussion of errors).

Intrinsic shape correlations are interesting in their own right, as they provide a probe to the generation of angular momentum during galaxy formation. Galaxy spins can for instance be used, in principle, to measure the shear of the density field (Lee & Pen 2000). The SuperCOSMOS, APM and SDSS surveys can thus be used to measure the intrinsic correlation functions with high accuracy. Intrinsic correlations can also be constrained using 2-dimensional galaxy-

galaxy lensing to measure the alignment of mass and light in galaxies (Natarajan & Refregier 2000). These techniques can then be used to constrain models of galaxy formation, and to secure the interpretation of deeper weak lensing surveys.

ACKNOWLEDGMENTS

The simulations analysed in this paper were carried out using data made available by the Virgo Supercomputing Consortium (<http://star-www.dur.ac.uk/~frazierp/virgo/>) using computers based at the Computing Centre of the Max-Planck Society in Garching and at the Edinburgh Parallel Computing Centre. We are very grateful to Rob Smith for providing halos from the simulations. We thank Rachel Somerville, Priya Natarajan and Rob Crittenden for useful discussions, and the referee for helpful comments. AR was supported by a TMR postdoctoral fellowship from the EEC Lensing Network, and by a Wolfson College Research Fellowship. Some computations used Starlink facilities.

REFERENCES

- Bacon D., Refregier A., Ellis R., 2000, submitted to MNRAS, preprint astro-ph/0003008
- Bartelmann M., Schneider P., 1999, submitted to Physics Reports, preprint astro-ph/9912508
- Bernardeau F., Van Waerbeke L., Mellier Y., 1997, *A&A*, 322, 1
- Blandford R.D., Saust A.B., Brainerd T.G., Villumsen J.V., 1991, MNRAS, 251, 600
- Catelan P., Theuns T., 1996a, MNRAS, 282, 436
- Catelan P., Kamionkowski M., Blandford R.D., 2000, *astro-ph* 0005470
- Crittenden R., Natarajan P., Pen U., Theuns T., 2000, in preparation
- Croft R.A.C., Metzler C.A., 2000, *astro-ph*/0005384
- Doroshkevich A.G., 1970, *Afz*, 6, 581
- Folkes S., et al, 1999, MNRAS, 308, 459
- Fort B., Mellier Y., 1994, *Astron. Astr. Rev.* 5, 239.
- Giavalisco M., Steidel C.C., Adelberger K.L., Dickinson M.E., Pettini M., Kellogg M., 1998, *ApJ*, 503, 543
- Heavens A.F., Peacock J.A., 1988, MNRAS, 232, 339
- Hoekstra H., Franx M., Kuijken K., 1999, in *Gravitational Lensing: Recent Progress and Future Goals*, ASP conference series, eds. Brainerd T., Kochanek C.S.
- Hoyle F., 1949, in Burgers J. M., van de Hulst H. C., eds., in *Problems of Cosmical Aerodynamics*, Central Air Documents, Dayton, Ohio, p. 195
- Gunn J.E., Weinberg D.H., 1995, in Maddox S., Aragon-Salamanca A., eds., in *Wide Field Spectroscopy and the Distant Universe, the 35th Herstmonceux Conference*, p.3
- Hu W., Tegmark M., 1998 (*astro-ph*/9811168)
- Jain B., Seljak U., 1997 *ApJ*, 484, 560
- Jenkins A., et al., 1998, *ApJ* 499, 20
- Kaiser N., 1992, *ApJ* 498, 26.
- Kaiser N., Squires G., 1993, *ApJ* 404, 441.
- Kaiser N., 1998, *ApJ* 498, 26.
- Kaiser N. et al., 1998, submitted to *ApJ*, preprint *astro-ph*/9809268
- Kaiser N., 1999a, Review talk for Boston 99 lensing meeting, preprint *astro-ph*/9912569
- Kaiser N., Wilson G., Luppino G.A., 2000, submitted to *ApJL*, preprint *astro-ph*/0003338
- Kamionkowski M., Babul A., Cress, C.M., Refregier A., 1997, MNRAS, 301, 1064, preprint *astro-ph*/9712030
- Lee J., Pen U.-L., 2000, *ApJ*, 532, L5
- Limber D.N., 1953 *ApJ* 117, 134.
- Maddox S.J., Sutherland W.J., Efstathiou G., Loveday J., 1990, MNRAS, 243, 692
- Lin H., Kirshner R.P., Shectman S.A., Landy S.D., Oemler A., Tucker D.L., Schechter P.L., 1996, *ApJ*, 464, 60
- Loveday J., Peterson, B.A., Efstathiou G., Maddox S.J., 1992, *ApJ*, 390, 338
- Mellier Y., 1999, *ARAA*, 37, 127
- Miralda-Escudé J., 1991, *ApJ*, 380, 1
- Munshi D., Coles P., 2000, *astro-ph*/0003481
- Natarajan P., Refregier A., 2000, to appear in *ApJL*, preprint *astro-ph*/0003344
- Navarro J.M., Steinmetz M., 1997, *ApJ*, 478, 13
- Peacock J.A., 1999, *Cosmological Physics*, (Cambridge University Press: Cambridge)
- Peacock J., Dodds S.J., 1997, MNRAS, 280, L19
- Peebles P.J.E., 1969, *ApJ*, 155, 393
- Pen U.-L., 1999, *ApJS*, 120, 49
- Pen U.-L., Lee J., Seljak U., 2000, submitted to *ApJL*, *astro-ph*/0006118
- Rhodes, J., Refregier A., Groth E., 1999, to appear in *ApJ*, *astro-ph*/9905090
- Schneider P., 1996 in *Universe at High Z*, eds. Martinez-Gonzalez E., Sanz J., p470.
- Schneider P., Van Waerbeke L., Jain B., Kruse G., 1998, MNRAS, 296, 893
- Smail I., Hogg D.W., Cohen J.G., 1995, *ApJ*, 449, L105
- Stebbins A., McKay T., Frieman J.A., 1995, in *Proc. IAU Symposium* 173, preprint *astro-ph*/9510012
- Sugerman B., Summers F.J., Kamionkowski M., 1999, submitted to MNRAS, *astro-ph*/9909266
- Tormen G., 1997, MNRAS, 290, 411
- Van Waerbeke L., Bernardeau F., Mellier Y., 1999, *A&A* in press, *astro-ph*/9807007
- Van Waerbeke L., et al. 2000, submitted to *A&A*, preprint *astro-ph*/0002500
- Villumsen J.V., 1996, MNRAS, 281, 369
- West M.J., Villumsen J.V., Dekel A., 1991, *ApJ*, 369, 287
- White S.D.M., 1984, *ApJ*, 286, 38
- Wittman D.M., Tyson J.A., Kirkman D., Dell'Antonio I., Bernstein G., 2000, submitted to *Nature*, preprint *astro-ph*/0003014

This paper has been produced using the Royal Astronomical Society/Blackwell Science L^AT_EX style file.